

# FLOURY ENDOSPERM16 encoding a NAD-dependent cytosolic malate dehydrogenase plays an important role in starch synthesis and seed development in rice

Xuan Teng<sup>1</sup>, Mingsheng Zhong<sup>1</sup>, Xiaopin Zhu<sup>1</sup>, Chunming Wang<sup>1</sup>, Yulong Ren<sup>2</sup>, Yunlong Wang<sup>1</sup>, Huan Zhang<sup>1</sup>, Ling Jiang<sup>1</sup>, Di Wang<sup>1</sup>, Yuanyuan Hao<sup>1</sup>, Mingming Wu<sup>1</sup>, Jianping Zhu<sup>1</sup>, Xin Zhang<sup>2</sup>, Xiuping Guo<sup>2</sup>, Yihua Wang<sup>1,\*</sup> and Jianmin Wan<sup>1,2,\*</sup> 

<sup>1</sup>State Key Laboratory for Crop Genetics and Germplasm Enhancement, Jiangsu Plant Gene Engineering Research Center, Nanjing Agricultural University, Nanjing, China

<sup>2</sup>National Key Facility for Crop Resources and Genetic Improvement, Institute of Crop Science, Chinese Academy of Agricultural Sciences, Beijing, China

Received 5 February 2019;

accepted 7 March 2019.

\*Correspondence (Tel +86-010-82105838;

fax +86-010-82105811; emails

wanjm@njau.edu.cn or

wanjianmin@caas.cn (J. W.);

yihuawang@njau.edu.cn (Y. W.)

## Summary

Starch is the most important form of energy storage in cereal crops. Many key enzymes involved in starch biosynthesis have been identified. However, the molecular mechanisms underlying the regulation of starch biosynthesis are largely unknown. In this study, we isolated a novel floury endosperm rice (*Oryza sativa*) mutant *flo16* with defective starch grain (SG) formation. The amylose content and amylopectin structure were both altered in the *flo16* mutant. Map-based cloning and complementation tests demonstrated that *FLO16* encodes a NAD-dependent cytosolic malate dehydrogenase (CMDH). The ATP contents were decreased in the mutant, resulting in significant reductions in the activity of starch synthesis-related enzymes. Our results indicated that *FLO16* plays a critical role in redox homeostasis that is important for compound SG formation and subsequent starch biosynthesis in rice endosperm. Overexpression of *FLO16* significantly improved grain weight, suggesting a possible application of *FLO16* in rice breeding. These findings provide a novel insight into the regulation of starch synthesis and seed development in rice.

**Keywords:** floury endosperm mutant, starch synthesis, grain weight, malate, energy supply, redox regulation, rice.

## Introduction

Starch, large biopolymers of glucose, is the most important form of carbohydrates for most organisms. As the major source of daily carbon intake for humans, starch has a vital role in our diet and health. Cereal endosperm accumulates high levels of starch that provides energy for seed germination and early seedling development. In rice (*Oryza sativa*), endosperm starch forms insoluble particles referred to as starch grains (SGs) in the amyloplasts. A SG is generally composed of a complex of sharp-edged polyhedral starch granules (Jane *et al.*, 1994), also named as compound SG (Tateoka, 1962). SGs are easily observed by staining with iodine solution using a light microscope.

Starch synthesis begins with the enzyme ADP-glucose pyrophosphorylase (AGPase) catalysing the reaction of glucose 1-phosphate (G1P) and ATP to ADP-glucose (ADPG), the substrate for starch synthesis (Martin and Smith, 1995). In contrast to most higher plants and leaves of cereal crops (Beckles *et al.*, 2001; Tetlow *et al.*, 2003), the major forms of AGPase in cereal endosperm are located in the cytosol (Tetlow *et al.*, 2003). Synthesized ADPG is then transported from the cytosol to amyloplasts by the ADPG transporter, Brittle 1 (Li *et al.*, 2017; Sullivan *et al.*, 1991). Five starch synthase (SS) isoforms synthesize and elongate glucan chains using ADPG as the substrate. Granule-bound starch synthase (GBSS) acts in biosynthesis of amylose and extra-long unit chains of amylopectin in rice (Hanashiro *et al.*, 2008), and other SS isoforms (SSI, SSII, SSIII and SSIV) participate in amylopectin biosynthesis (Nakamura, 2002). Branching enzymes (BEs) and debranching enzymes (DBEs) are required to define amylopectin structure (Ball *et al.*, 1996). In

addition to the enzymes mentioned above, additional factors indirectly regulate starch synthesis. For example, Du1 regulates starch synthesis by assisting the splicing of *waxy* pre-mRNA (Isshiki *et al.*, 2000). Previous study in wheat revealed that protein phosphorylation regulates activity and integrity of a protein complex formed by BEIIb, BEI and plastidial phosphorylase (PHO1) (Tetlow *et al.*, 2004). Evidence for interaction between BEII, SSI and SSII was also obtained in developing wheat endosperm (Tetlow *et al.*, 2008). However, detailed starch biosynthesis mechanisms, especially their regulation, are far from complete resolution.

Opaque-kernel mutant phenotypes indicate changes in storage metabolites, varying starch content and structure, aberrant SGs, and other abnormalities. Various rice mutants with opaque endosperm and individual SGs were named floury, including *flo(a)* (Qiao *et al.*, 2010), *flo2* (She *et al.*, 2010), *flo3* (Nishio and Iida, 1993), *flo4* (Kang *et al.*, 2005), *flo5* (Ryoo *et al.*, 2007), *flo6* (Peng *et al.*, 2014), *flo7* (Zhang *et al.*, 2016) and *flo8* (Long *et al.*, 2017). Some mutants with abnormal SGs were named as *sub-standard starch grain* (*ssg1-6*) (Matsushima *et al.*, 2010, 2014, 2016), *dull* (*du1-3*) (Isshiki *et al.*, 2000, 2008; Zeng *et al.*, 2007) and *chalk5* (Li *et al.*, 2014). All previous studies confirmed that defective endosperm mutants are valuable genetic resources for dissecting the mechanisms of amyloplast development and starch biosynthesis.

Malate content contributes to redox homeostasis in the cytosol. Malate participates in the transport of redox equivalents among cell compartments (Kromer and Scheibe, 1996; Scheibe, 2004). In tomato, malate was identified as a potential metabolite regulating starch synthesis. Further analysis suggested that an

altered plastidial redox status caused by modified malate metabolism resulted in different AGPase activation states and final starch contents (Centeno *et al.*, 2011). Similar conclusions were made for potato (Tiessen *et al.*, 2002). However, in potato tubers, starch synthesis in plastids was not affected by decreased synthesis of malate in mitochondria, suggesting that redox regulation is tissue dependent (Szecowka *et al.*, 2012). However, the role that malate metabolism plays in starch synthesis in rice endosperm remains unknown.

In this study, a flourey mutant, *flo16*, with a deletion of 4 base pairs in the *Cytosolic Malate Dehydrogenase* gene was isolated and characterized. Compared to the wild type, decreased starch and increased sucrose contents in the *flo16* mutant revealed that the transition from sucrose to starch was partially disrupted during mutant grain filling. Endosperm-specific overexpression of *FLO16* led to increased grain weight. Our results demonstrated that *FLO16* is important for starch biosynthesis and seed development in rice.

## Results

### *flo16* endosperm is defective in starch accumulation

As part of our ongoing effort to dissect mechanisms underlying starch biosynthesis and its regulation in rice, we isolated a flourey endosperm mutant named *flo16* from a  $^{60}\text{Co}$ -irradiated  $M_2$  population of *indica* rice variety N22. The mature grains of *flo16* were opaque and slightly shrunken compared with the transparent and fully developed grains of wild type (Figure 1a,b). During endosperm development, the *flo16* mutant underwent a much slower grain-filling rate from 6 days after flowering (DAF), and this difference was maintained until maturation (Figure 1e). The 1000-grain weight of *flo16* was significantly lower than that of wild type (Figure 1f); and the grain thickness of *flo16* was smaller than that of the wild type (Figure 1g). Clearly, the *flo16* mutation affects starch accumulation during endosperm development. It is worth noting that the plant height of the *flo16* mutant was also shorter in height and had less tillers compared to wild type (Figure 1c,d; Table S1). These results suggest that the *flo16* mutant is also defective in plant growth and development and that changes in starch metabolism extend beyond the endosperm.

### *flo16* endosperm has irregular starch grain morphology

Semi-thin sections of developing endosperm in *flo16* at 12 DAF examined after iodine staining had massive unstained spaces apparently caused by delayed filling of amyloplasts (Figure 2c,d). Amyloplasts in wild-type endosperm were full of densely packed compound SGs consisting of polyhedral granules (Figure 2a,b), whereas in *flo16* endosperm they were tiny and disordered (Figure 2c,d). Besides compound SGs, many single granules were scattered in the mutant endosperm (Figure 2d). Scanning electron microscopy (SEM) of transverse sections of mature endosperm revealed that, unlike the regular, compact crystal structure of wild-type SGs (Figure 2e–g), the endosperm of *flo16* consisted of small, spherical and loosely packed SGs with large air spaces (Figure 2h–j). Therefore, formation of compound SGs was severely disrupted in developing *flo16* endosperm.

### Physicochemical properties of *flo16* starch

Total starch and amylose contents in dry weight of mature *flo16* seeds were significantly less than in wild-type seeds (Figure 3a,b), whereas protein and lipid contents were both elevated

(Figure 3c,d). Sucrose content in *flo16* endosperm was 8 times higher than in the wild type (Figure 3e), suggesting disruption of transition from sucrose to starch. Although amylopectin content taken up in mature *flo16* seeds was almost unchanged, the degrees of polymerization (DP) in the ranges 6–10 and 13–14 were significantly increased, whereas those in the ranges of DP 11–12 and DP 15–48 were decreased (Figure 3f). There were no visible alterations in the amounts of A-chains with DP 6–12 and B-chains with DP > 36 as classified by Hanashiro *et al.* (2002). However, elongation of both A-chains and B-chains was abnormal in the *flo16* mutant (Figure 3f). The solubility of starch in urea solution was measured to test the gelatinization properties (Nishi *et al.*, 2001). Even in 9 M urea powdered *flo16* starch was difficult to gelatinize, whereas wild-type starch began to gelatinize in 5 M urea and was thoroughly gelatinized in 9 M urea (Figure 3g). Analyses of pasting properties revealed that the viscosity of *flo16* pasting starch was low after the rise in temperature, but the curve patterns showed no difference between wild type and *flo16* (Figure 3h). Collectively, the physicochemical properties of *flo16* starch were significantly altered compared with the wild type.

### The *flo16* mutation occurred in gene *Os10 g0478200*

When *flo16* was crossed with wild type, approximately one-quarter of the  $F_2$  seeds had flourey endosperm (296 of 1,205,  $\chi^2_{3:1} = 0.122 < \chi^2_{0.05,1} = 3.84$ ), indicating that the mutant phenotype was inherited as a single recessive allele. We then undertook map-based cloning to identify the underlying gene. First, 10 individuals with flourey endosperm selected from the  $F_2$  progeny of cross *flo16* (*indica*)  $\times$  DJY (*japonica*) were used for linkage detection. The *FLO16* locus was initially mapped between markers I10-6 and 10-26 on the long arm of chromosome 10. Then, 125 *flo16* individuals were used to position *FLO16* between markers H188-15 and H188-2. Finally, 1,502 individuals with the recessive phenotype reduced the position of *FLO16* to an 88 kb region between markers 188–21 and 188–2 (Figure 4a; Table S3). Six predicted open reading frames (ORFs) in the region were sequenced, and we found a deletion of 4 base pairs in the coding region of *Os10 g0478200*, leading to a frame shift from amino acid residue 229 (Figure 4b), and a premature termination codon. *Os10 g0478200* was predicted to encode a cytosolic malate dehydrogenase (CMDH) composed of 332 amino acids.

To verify the identity of *flo16*, we cloned the genomic sequence of *FLO16* starting from 2,000 nucleotides upstream of the putative starting codon (ATG) to the stop codon (TAA) of *Os10 g0478200* into a plant expression vector, which was then introduced into *flo16*. Seed and SG morphologies of positive transgenic plants were similar to wild-type plants, indicating successful rescue of the defects caused by the *flo16* mutation (Figure 4c–f). Therefore, *Os10 g0478200* was confirmed to be the gene responsible. In addition, we generated transgenic lines expressing *CMDH* driven by *Glutelin C* promoter in *flo16*, and the endosperm-specific expression of *CMDH* rescued the phenotype of the mutant (Figure S1), indicating that the mutant phenotype in *flo16* was mainly due to the defects in seeds rather than in vegetative tissues.

### *FLO16* is cytosol-located protein that is ubiquitously expressed in rice

We performed quantitative RT-PCR (qRT-PCR) analyses in wild-type plants to investigate the expression profile of *FLO16*.

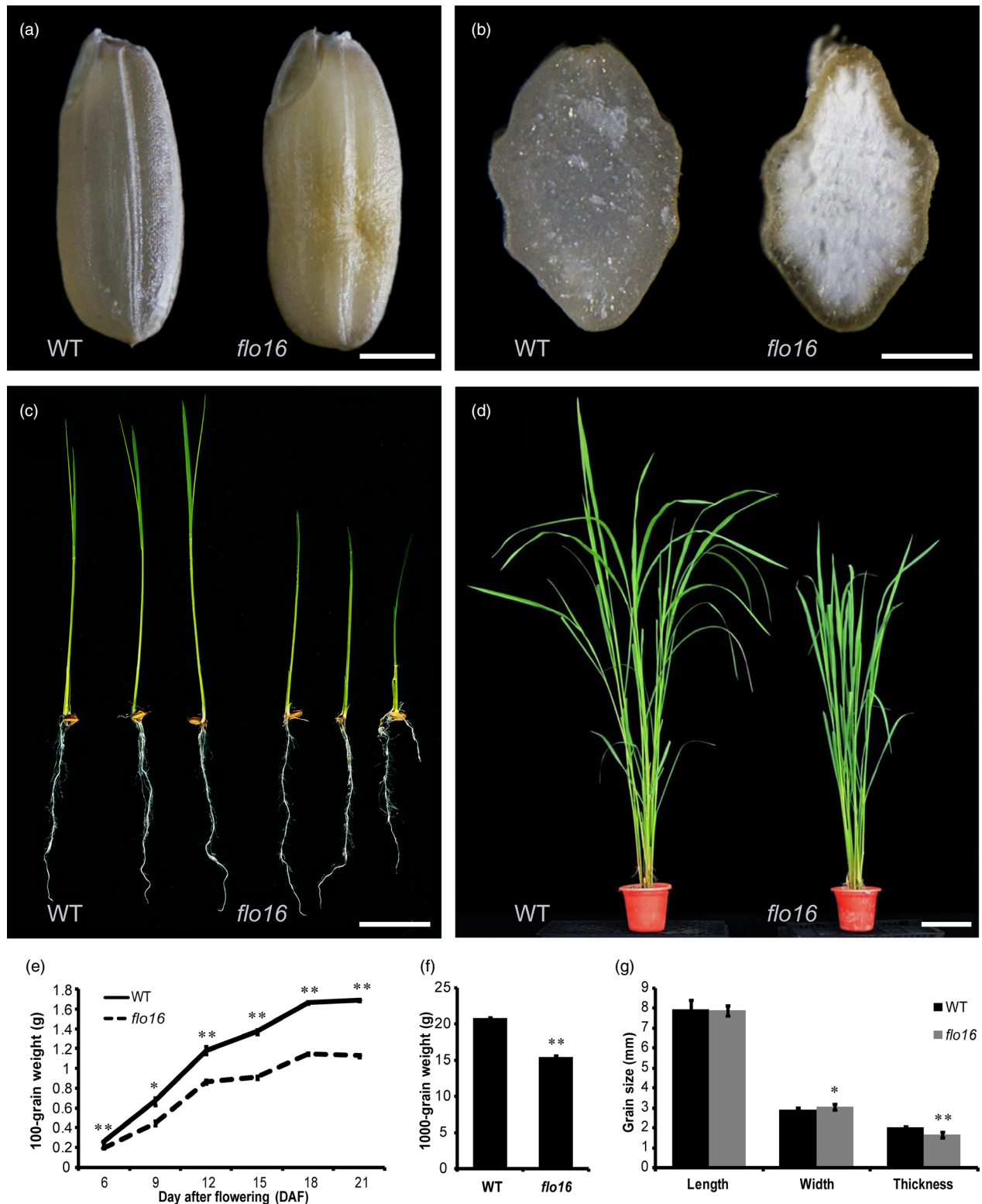


**Figure 1** Phenotypes of the *flo16* mutant. (a) Images of mature seeds of wild type (left) and *flo16* (right). Scale bar, 2 mm. (b) Cross sections of the mature seeds of wild type (left) and *flo16* (right). Scale bar, 1 mm. (c) One-week-old seedlings of wild type (left) and *flo16* (right). Scale bar, 4 cm. (d) Wild type (left) and *flo16* (right) plants at the booting stage. Scale bar, 20 cm. (e) Grain weights of wild type and *flo16* at various stages post-fertilization. Grain weight indicates the weight of 100 dehulled dry grains, values are means  $\pm$  SD,  $n = 3$ . (f) 1000-grain weights of wild type and *flo16*. Values are means  $\pm$  SD,  $n = 5$ . (g) Grain size comparisons between wild type and *flo16*. Values are means  $\pm$  SD,  $n = 10$ . Asterisks indicate the statistical significance between the wild type and mutants determined by Student's *t*-tests (\* $P < 0.05$ ; \*\* $P < 0.01$ ).



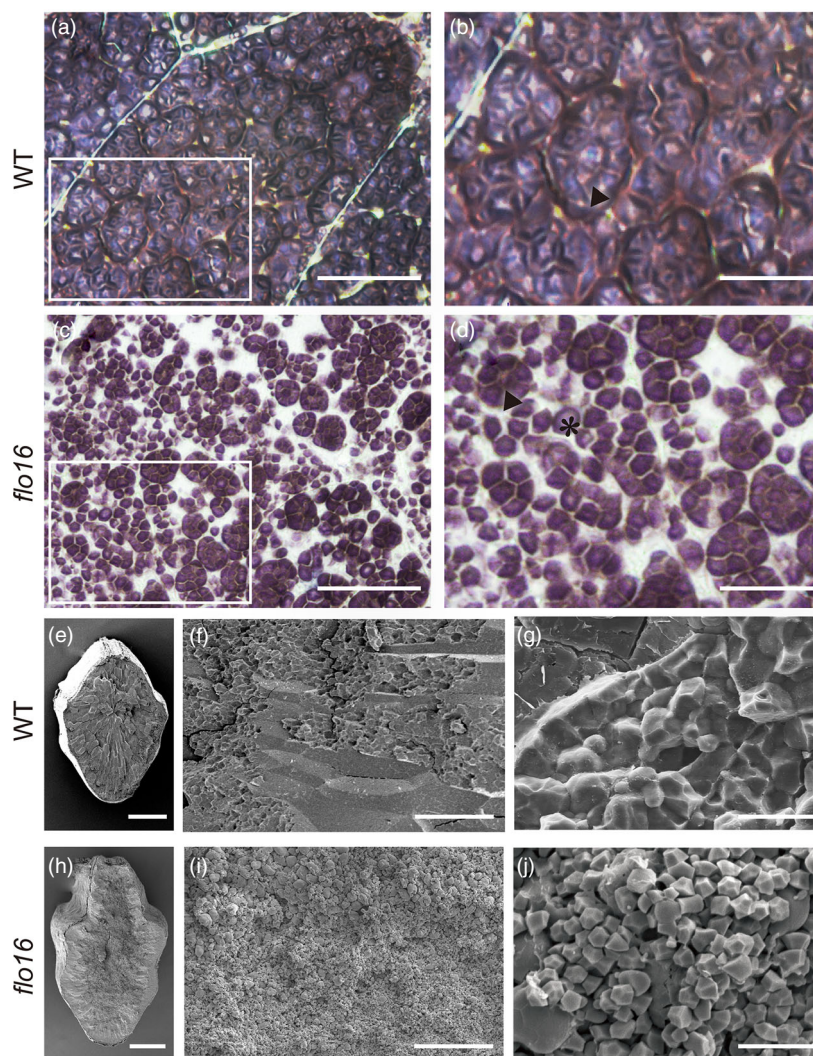


**Figure 2** Abnormal starch grain (SG) formation in *flo16* endosperm. (a–d) Semi-thin sections of the wild type (a, b) and *flo16* (c, d) endosperms at 12 days after flowering (DAF). (b) and (d) are enlargements of the boxed areas in (a) and (c), respectively. Small and scattered SGs are displayed in lower left of (b, d). Triangles indicate compound starch grains in (b) and (d); a asterisk indicates a single starch grain in (d). (e–j) SEM of endosperm of wild type (e–g) and *flo16* (h–j). Scale bars, 40  $\mu\text{m}$  in (a, b), 20  $\mu\text{m}$  in (c, d), 1 mm in (e, h); 200  $\mu\text{m}$  in (f, i); 10  $\mu\text{m}$  in (g, j).

Expression levels of *FLO16* in vegetative tissues, especially leaf sheaths and panicles, were higher than in the developing endosperm. Expression of *FLO16* during endosperm development increased at 6–15 DAF, but reduced at 18 DAF (Figure 5a). Hence, *FLO16* expression occurs in the early and mid-endosperm development stages, corresponding with the time of starch biosynthesis. GUS staining in transgenic lines carrying a  $\beta$ -glucuronidase (*GUS*) expression vector driven by the *FLO16* promoter confirmed that *FLO16* was ubiquitously expressed in rice. *FLO16* also showed a relatively high level of expression in anthers, early developing grains and stem nodes, and had a spotty distribution in leaves (Figure 5b–j). Constitutive expression suggested that functions of *FLO16* might not be limited to the endosperm.

The *FLO16* gene was predicted to encode a cytosolic protein. To verify the subcellular location, the coding sequence of *FLO16* was C-terminally fused with *GFP* driven by the cauliflower mosaic virus 35S (CaMV35S) promoter. Free GFP in the control was diffused evenly in cytoplasm (Figure 5k lower panel). The distribution pattern of the *FLO16*-GFP signal (Figure 5k upper panel) was almost the same as that of free GFP, suggesting that *FLO16* protein was diffused in the cytosol as predicted.

### Disruption of *FLO16* causes multiple metabolic changes

MDH isoforms catalyse the reversible conversion of malate to OAA (Gietl, 1992; Heber, 1974; Scheibe, 2004). To determine endogenous MDH activity, crude enzyme was extracted from developing endosperm 6 and 9 DAF for native polyacrylamide gel electrophoresis (PAGE) analysis. As expected, one of the activity bands was not detected in the *flo16* mutant, which was recovered in the complementation lines. Thus, *flo16* seems to be a knockout mutant of CMDH. Interestingly, other activity bands showed a slight compensatory increase (Figure 6a). The total NAD-MDH activity in *flo16* endosperm at 9 DAF was less than one-half of that in the wild type (Figure 6b). The lack of CMDH activity might result in alterations in substrates and products of malate metabolism. We evaluated the levels of closely related metabolites. There was an increase in malate levels in young leaves and roots relative to wild type, and malate levels in grains were increased only at 9 DAF (Figures S3A and 6c). We inferred that malate was mainly the substrate of CMDH. Considering that a 'malate valve' plays an essential role in redox regulation and energy conversion (Scheibe, 2004), we evaluated the major form of redox power and energy supplying, and identified decreases in the NADPH and ATP content (Figure S2).



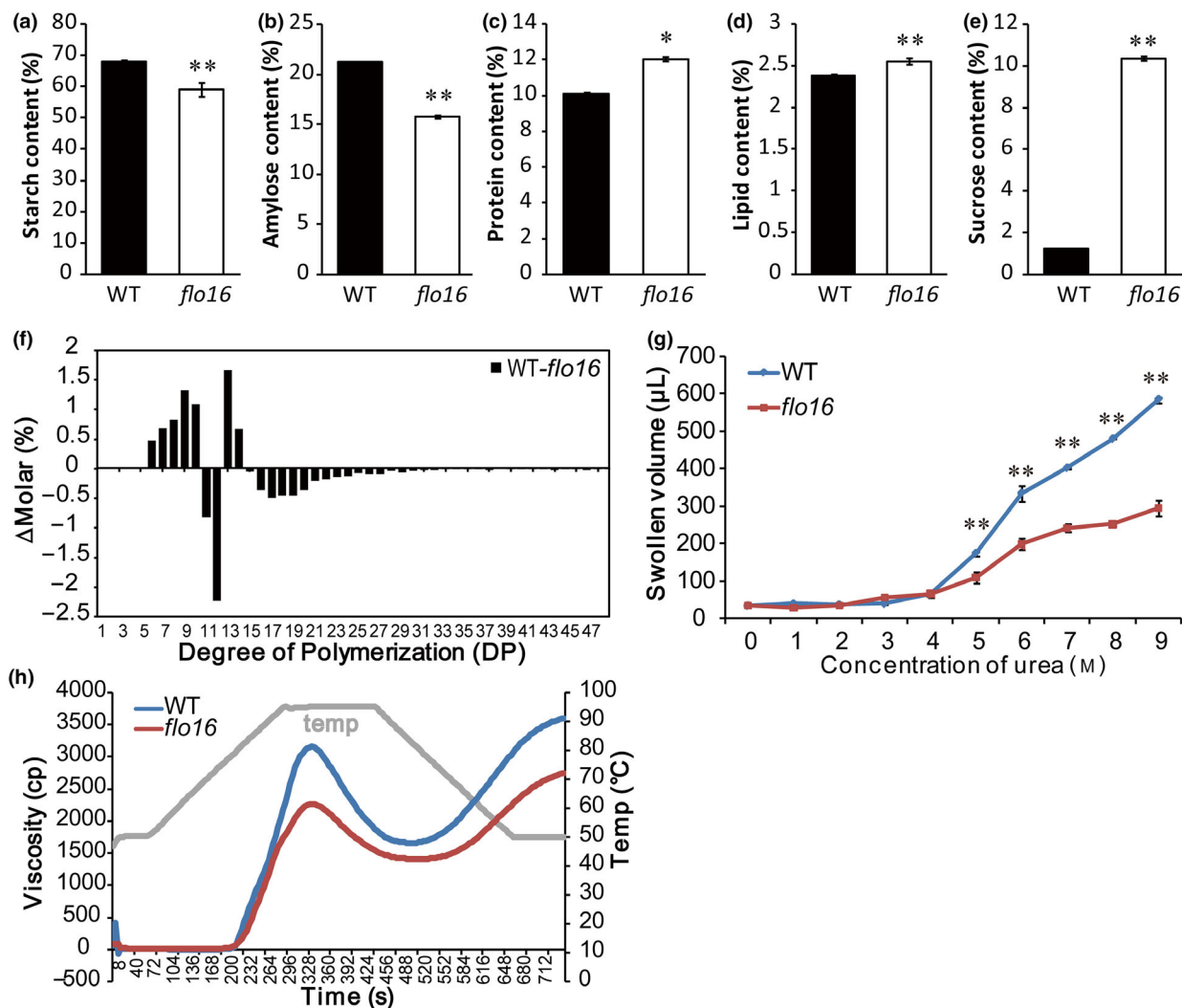


**Figure 3** Properties of grains and physicochemical characteristics of starch in the *flo16* mutant. (a–e) The contents of total starch (a), amylose (b), protein (c), lipid (d) and sucrose (e) were proportions of grain dry weight in wild type and *flo16*. Values are means  $\pm$  SD,  $n = 3$ . (f) Differences in amylopectin chain length distributions between the wild type and the *flo16* mutant. (g) Swollen volumes of wild-type and *flo16* starch in urea solutions at various concentrations (0–9 M). Values are means  $\pm$  SDs,  $n = 3$ . (h) Pasting properties of endosperm starch of the wild type and *flo16* mutant. Grey line indicates temperature changes during measurements. Asterisks indicate the statistical significance between the wild type and mutant determined by Student's *t*-tests (\* $P < 0.05$ ; \*\* $P < 0.01$ ).

This indicated that energy metabolism and redox homeostasis were unstable in the *flo16* mutant.

#### Defective starch biosynthesis in *flo16*

Sucrose contents in single developing and mature grains of *flo16* were much higher than in the wild type (Figure 6d), while starch contents were obviously lower (Figure 6e). Real-time quantitative RT-PCR was performed to examine possible effects of FLO16 on starch biosynthesis. Expression levels of many genes participating in starch biosynthesis during endosperm development were decreased, including genes coding for UDPG pyrophosphatase (UGPase), AGPases (AGPL2 and AGPS2b), soluble SSI (SSI), GBSSI, BEI, BEIIb, isoamylases (ISA1 and ISA2) and pullulanase (PUL). In contrast, genes coding for cytosolic phosphorylase (PHO2), disproportionating enzyme (DPE1 and DPE2) and sucrose synthase (Susy3) were increased, whereas

FLO2, PPKB (*Pyruvate orthophosphate dikinase B*) and RSR1 (*Rice starch regulator 1*) were only slightly increased (Figure 7a). It seems that genes functioning upstream of AGPase were highly expressed, and those acting downstream of AGPase were significantly reduced.

The activities of key enzymes in starch synthesis were investigated. We first investigated AGPase activity since it was the rate-limiting enzyme in starch synthesis. As predicted, AGPase activity in developing *flo16* endosperm was lower than in the wild type (Figure 7b). Zymogram analyses performed to detect activities of several essential starch synthetic enzymes showed decreased activities of SSI (Figure 7c) and PHO1 (Figure 7d) in the *flo16* mutant relative to wild type, but there was no significant change in SSIII and PHO2 activity. Thus, mutation of the FLO16 gene showed obvious effects on the activities of the key starch synthetic enzymes.

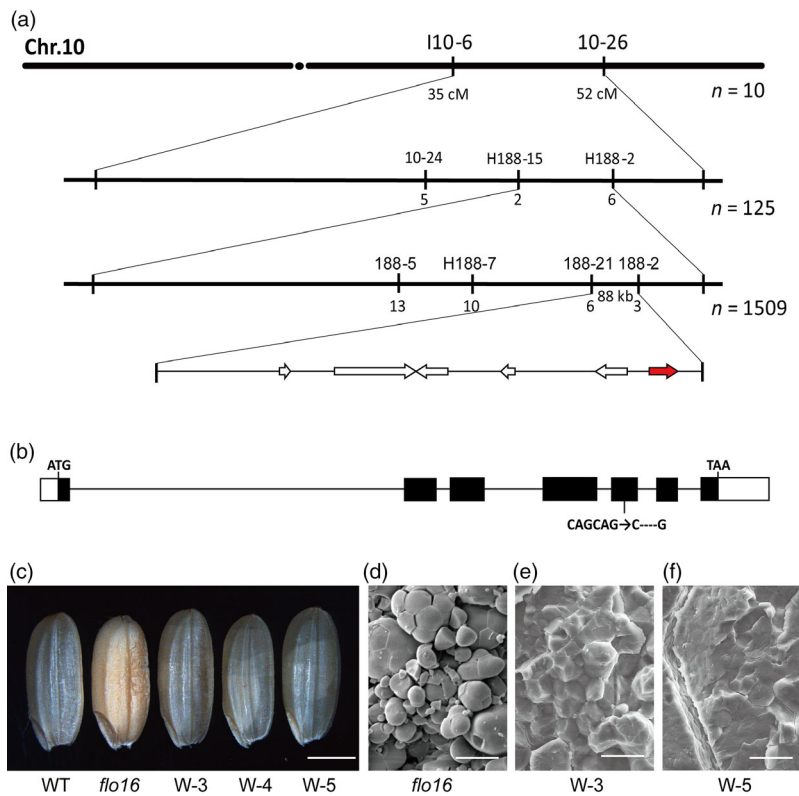


**Figure 4** Map-based cloning of *FLO16*. (a) Fine mapping of the *FLO16* locus. The *FLO16* locus was mapped to an 88 kb region by markers 188–21 and 188–2 on chromosome 10 (Chr.10), containing six predicted genes. Numbers of recombinants are indicated below the map. (b) The *flo16* mutant has a 4 bp deletion in the fifth exon of *Os10g0478200*. White boxes indicate untranslated regions; black boxes indicate exons; lines indicate the introns. (c–f) Functional complementation lines of *flo16* restore normal seed appearance. Complemented seeds became translucent (c), and SGs were restored to normal (d–f). W-3, W-4 and W-5 are representative positive transgenic lines. Scale bars, 2 mm in (c), 25  $\mu$ m in (d–f).

### Starch biosynthesis in *flo16* has almost no response to exogenous malate or sucrose

Alterations in malate level caused dramatic effects on transitory starch metabolism in tomato fruit (Centeno *et al.*, 2011). However, no difference in starch content was observed when malate level was decreased in potato (Szecowka *et al.*, 2012). We investigated the influence of malate on starch synthesis in the developing endosperm of rice. Isolated *flo16* and wild-type endosperms at 9–12 DAF were incubated in the presence of 0, 5 or 125 mM malate for 3 h, respectively. Endosperm discs were washed twice, and the activities of starch synthesis-related enzymes were determined. Catalytic activity of AGase in the wild type was induced by malate treatment, whereas that in *flo16* was significantly lower and barely responded to malate treatment (Figure 8a). Concurrently, expression levels of several key enzymes in starch synthesis were tested for induction in wild-type endosperm (Figure 8b). Those experiments revealed up-regulation in starch biosynthetic flux, suggesting that exogenous malate promoted transition from sucrose to starch. The deletion of *CMDH* at least partly blocked the response of starch synthesis to malate. Similar results were obtained when developing endosperms of *flo16* and wild type were treated with sucrose (Figure 8c). Thus, the starch synthesis in *flo16* mutant is defective in response to exogenous malate and sucrose.

### Overexpression of *FLO16* increases grain weight

We created transgenic lines overexpressing *FLO16* driven by the endosperm-specific *Glutelin C* promoter to evaluate the effect of elevated *FLO16* expression level in rice endosperm. qRT-PCR analysis showed that the expression levels of *FLO16* in positive transgenic lines were much higher than those in the endosperm

of the recipient cultivar Zhonghua 11 (Figure 9c). The major agronomic traits of these transgenic plants showed almost no difference with the recipient (Table S2). Notably, the 1000-grain weight of these lines were significantly higher than Zhonghua 11 (Figure 9g), indicating that endosperm-specific overexpression of *CMDH* will significantly promote starch biosynthesis in rice. Further analysis showed the elevated grain weight are mainly to the enlarged grain size as the grain length of transgenic lines were much larger than Zhonghua 11 (Figure 9a, d). This trend was even more obvious when dehulled grains were compared (Figure 9b). It is noteworthy that constitutive overexpression of *CMDH* could also result in increased grain weight (Figure S5).

## Discussion

### *CMDH* has strong effects on starch biosynthesis during seed development

Previous studies characterized several mutants that affected starch synthesis in rice. Many of them have opaque endosperm, such as *flo5* (*ssl1a*), *waxy* (*gbss1*) and *amylose-extender* (*ae*, *bellb*) (Nishi *et al.*, 2001). Endosperm-defective mutants are valuable resources for elucidating molecular mechanisms underlying seed development and/or starch biosynthesis. In this study, we isolated mutant *flo16* with floury endosperm and retarded growth. Its opaque endosperm appearance seemed to be caused by defective SG formation (Figure 2). Further analyses revealed that reduction in starch synthesis in *flo16* endosperm led to reduced grain weight (Figure 1f), and changes in amylose content and amylopectin structure (Figure 3a,b).

The *FLO16* locus was located within an 88 kb region in chromosome 10S. Sequence analysis and subsequent complementation tests determined that the underlying gene was

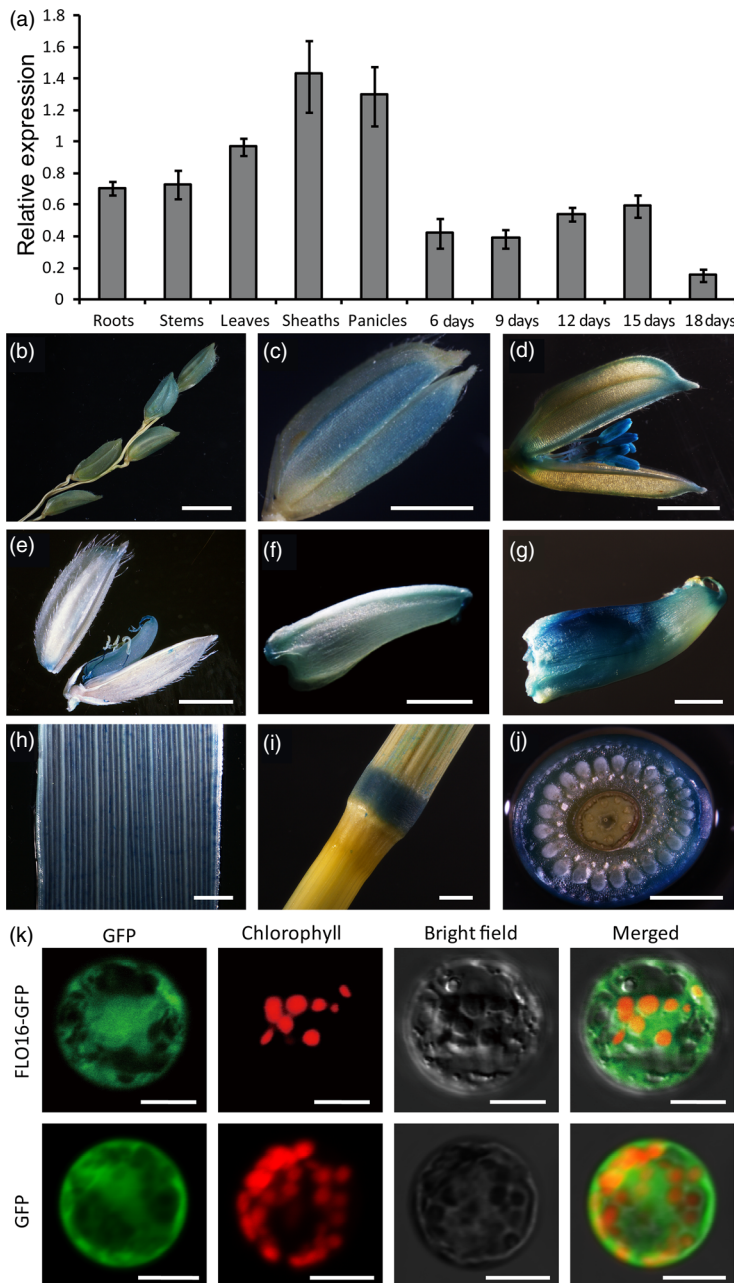


**Figure 5** Spatial expression patterns of *FLO16*. (a) Expression levels of *FLO16* in various tissues. Developing seeds were sampled at 6, 9, 12, 15 and 18 days after flowering (DAF), and other tissues were sampled at heading. The value of *Actin 1* mRNA was used as an internal control for data normalization. Values are means  $\pm$  SD,  $n = 3$ . (b–g) GUS activity in panicles (b), spikelet before heading (c), during heading (d), and at 3 DAF, and grains at 3 (e), 6 DAF (f) and 9 DAF (g), leaf (h), node (i, j). (j) Cross section of the node in (i). Scale bars, 10 mm in (b), 2 mm in (c–j). (k) Subcellular localization of *FLO16*. Free GFP served as a control (lower panel). The fusion construct *FLO16-GFP* was expressed in the rice protoplasts (upper panel). Green fluorescence signals, red chlorophyll autofluorescence, and bright field and merged images are shown in each panel. Scale bars, 10  $\mu$ m.

*Os10 g0478200*. A 4 bp deletion caused premature termination of *FLO16*, indicating that *flo16* is most probably a knockout mutant of that gene (Figure 4). MDH activity assays confirmed this result (Figure 6a). *Os10 g0478200* encodes a cytosolic malate dehydrogenase (CMDH) that is expressed ubiquitously. Expression of *CMDH* driven by endosperm-specific *Glutelin C* and *Ubiquitin* promoters both rescued the opaque phenotype of mutant seeds, indicating that the grain phenotype is due to lack of CMDH in the endosperm. Therefore, CMDH is important for starch biosynthesis during seed development.

#### CMDH functions in supplying reducing power and energy for starch biosynthesis in rice endosperm

Plant MDHs function in equilibrating reducing equivalents between organelles in the cell, and catalyse reversible conversion of malate and NAD(P) to OAA and NAD(P)H. In the cytosol,

malate is oxidized to oxaloacetate by the cytosolic MDHs, generating reducing equivalent in the form of NADH. Oxaloacetate is then transported to the plastids, where the plastidial MDH converts it back to malate. This so-called 'malate valve' is vital in equilibrating reducing equivalents in the cytosol and between organelles as well as regulating malate for further metabolic synthesis (Scheibe, 2004; Taniguchi and Miyake, 2012). An *Arabidopsis* double mutant lacking both the mitochondrial MDH isoforms was defective in seed maturation and post-germination growth (Sew *et al.*, 2016; Tomaz *et al.*, 2010), while the mutant deficient in peroxisomal isoforms requires exogenous sugars for seedling (Pracharoenwattana *et al.*, 2010). Plastidial NADP-MDH can be redox-regulated and activated dependent on light (Scheibe, 1987), while plastidial NAD-MDH is not redox sensitive and acts in dark and non-green parts (Berkemeyer *et al.*, 1998). Plant growth of *Arabidopsis nadp-mdh* mutants was either not



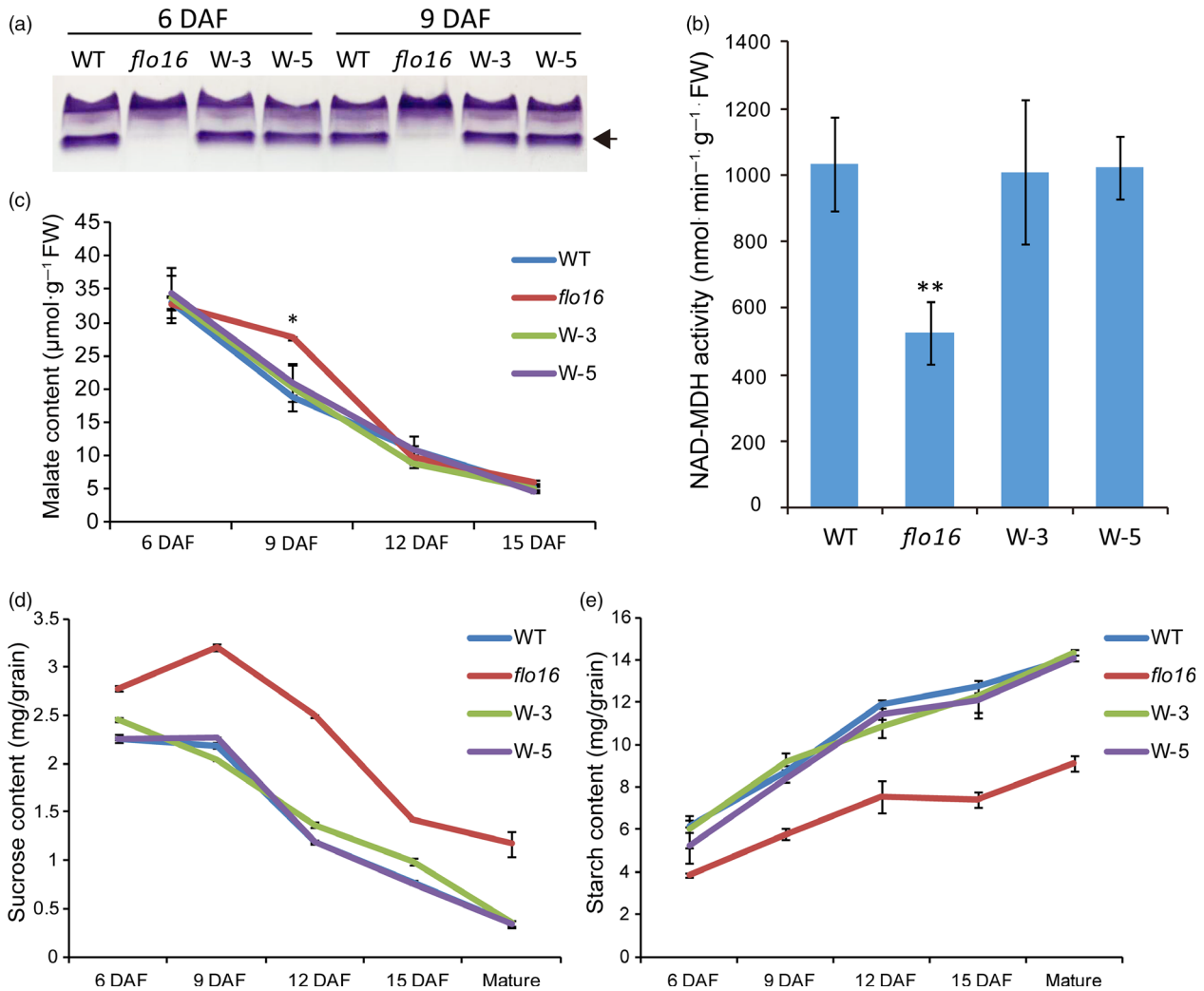


**Figure 6** Responses of the metabolic pathways to deletion of FLO16 activity. (a) Native PAGE profiles of malate dehydrogenase (MDH) activities in developing endosperms at 6 and 9 DAF. (b) Malate contents in developing endosperms. (c) NAD-MDH activity in wild-type and *flo16* developing endosperm. (d) Sucrose contents in developing and mature endosperm. (e) Starch contents in wild-type and *flo16* endosperm. All values are means  $\pm$  SD,  $n = 3$ . Asterisks indicate statistical significance between the wild type and mutant, determined by Student's *t*-tests (\* $P < 0.05$ ; \*\* $P < 0.01$ ).

affected (Hebbelmann *et al.*, 2012) or slight weakened (Heyno *et al.*, 2014) compared to the wild type, while *pdnad-mdh* knockout mutant has an embryo-lethal phenotype (Beeler *et al.*, 2014). Although it is well established that MDHs play important roles in central metabolism in plants, no *mdh* mutants were reported in rice. Recently, Heng *et al.* (2018) revealed that the defect in malate transport results in apical abortion panicles, suggesting an important role of malate metabolism in rice. However, the importance of CMDH in rice remains unclear.

In this study, CMDH activity was not detected in the *flo16* mutant, resulting in overaccumulated malate and decreased NADPH and ATP contents (Figures 6c and S2). This result suggested that rice CMDH mainly functions in converting malate and NAD(P) to OAA and NAD(P)H. Further exogenous malate treatment indicated that high levels of malate had no detrimental effect on starch biosynthesis (Figure 8a,b). Sucrose flux is the main form of substrate supply for starch synthesis in the endosperm. Exogenous sucrose in sweet potato increased the transcript level of *GBSSI* (Wang *et al.*, 2001). In our study, expression levels of *GBSSI* and several key enzymes in the wild type were induced by

sucrose and malate, whereas no significant differences were observed in *flo16* (Figure 8), indicating that starch synthesis in response to malate and sucrose is blocked in the *flo16* mutant. Starch synthesis requires a high rate of turnover of reducing equivalents and a mass of energy supply. Previous study in tomato showed that alterations in mitochondrial malate metabolism have strong effects on starch biosynthesis in the amyloplast due to an altered cellular redox status (Centeno *et al.*, 2011). In *flo16*, significantly decreased NADPH content indicated a lack of reduction potential required for starch synthesis. Moreover, ATP is referred to as the energy currency of the cell. Lower level of ATP in *flo16* is expected to result in a shortage of energy, which in turn greatly affects starch biosynthesis. Therefore, it is likely that alterations in cytosolic malate-related metabolism have strong effects on starch biosynthesis during seed development. Notably, mutation of CMDH led to defective plant growth, increased malate and reduced ATP content in *flo16* seedling, indicating that the malate-related metabolism also existed in other part of rice plant (Figures 1c,d and S3). However, the endosperm-specific expression of *CMDH* almost completely rescued these deficiencies.

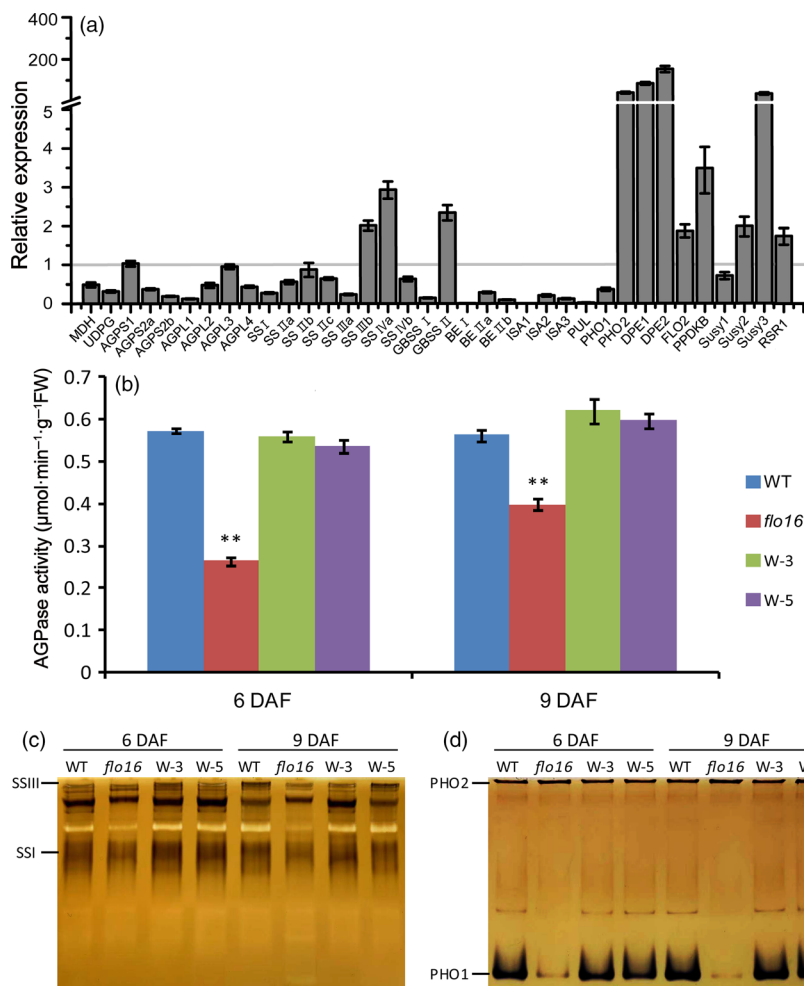


**Figure 7** Gene expression and protein activity analyses of starch synthesizing enzymes. (a) Expression levels of starch synthesis-related enzymes in developing endosperm 10 DAF. Data represent ratios of expression levels in *flo16* to that of wild type. Values are means  $\pm$  SD,  $n = 3$ . (b) AGPase activities in developing endosperm of wild type and *flo16*. Values are means  $\pm$  SD,  $n = 3$ . Asterisks indicate the statistical significance determined by Student's *t*-tests (\* $P < 0.05$ ; \*\* $P < 0.01$ ). (c) Activity bands for SSI, and SSIII. (d) Activity bands for PHO1 and PHO2.

Considering the significant role of photosynthesis in regulating redox state, we thus speculated that CMDH is more important in sink organs than source organs in rice.

Previous study in potato declared that the redox state affects starch synthesis by post-translational regulation of AGPase (Tiessen *et al.*, 2002). Moreover, the redox control of AGPase activity was also reported in rice endosperm (Tuncel *et al.*, 2014). However, our study clearly indicates that AGPase activity is independent of redox control as the decrease ratio was constant (Figure S4). Whether and how reducing equivalents alter the redox state of other starch synthesis-related enzymes remains to be further addressed.

### Overexpression of *FLO16* increases grain weight in rice

Grain weight is the major component of crop yield and an important agronomic trait in the breeding of cereal crops. Grain weight is positively associated with grain size. Several genes affecting grain weight have been identified in rice, such as *GS3* (Fan *et al.*, 2006; Mao *et al.*, 2010), *GW2* (Song *et al.*, 2007), *qSW5/GW5* (Liu *et al.*, 2017; Shomura *et al.*, 2008; Weng *et al.*, 2008), *GS5* (Li *et al.*, 2011), *qGL3/qGL3.1* (Qi *et al.*, 2012; Zhang *et al.*, 2012), *GW8* (Wang *et al.*, 2012), *TGW6* (Ishimaru *et al.*, 2013), *GL7/GW7* (Wang *et al.*, 2015a,b), *Gn1a* (Ashikari *et al.*, 2005), *DEP1* (Huang *et al.*, 2009) and *OsSPL14* (Jiao *et al.*, 2010), but the mechanisms that control grain weight are rarely reported.

Our endosperm-specific overexpressing of *CMDH* in Zhonghua 11 significantly increased grain weight which might due to the elevated grain length, demonstrated that elevated *CMDH* activity in the endosperm significantly promotes starch biosynthesis. Therefore, *FLO16* has the potential for improving grain weight and grain yield in rice.

## Experimental procedures

### Plant materials and growing conditions

The *flo16* mutant was generated by  $^{60}\text{Co}$  treatment of *indica* cv. N22 (Nagina22, an Indian traditional variety). An  $F_2$  population from cross *flo16* mutant  $\times$  *japonica* cv. DJY (Dianjingyou 1, from Yunnan Academy of Agricultural Sciences, *Japonica* Rice Breeding Center) was developed for fine mapping. Rice plants were grown in experimental fields at Nanjing or Beijing. Developing seeds of the wild type (N22) and *flo16* at 6–21 days after flowering (DAF) were harvested and stored at  $-80^\circ\text{C}$  if not used immediately.

### Starch grain observation

Transverse sections ( $\sim 1$  mm in thickness) of developing endosperm were fixed in 2% (W/V) paraformaldehyde, 2% (V/V) glutaraldehyde and 250 mM sucrose buffered with 50 mM PIPES-KOH (pH 7.2). The fixed endosperm was then dehydrated in an ethanol series and embedded in LR White resin (London Resin,

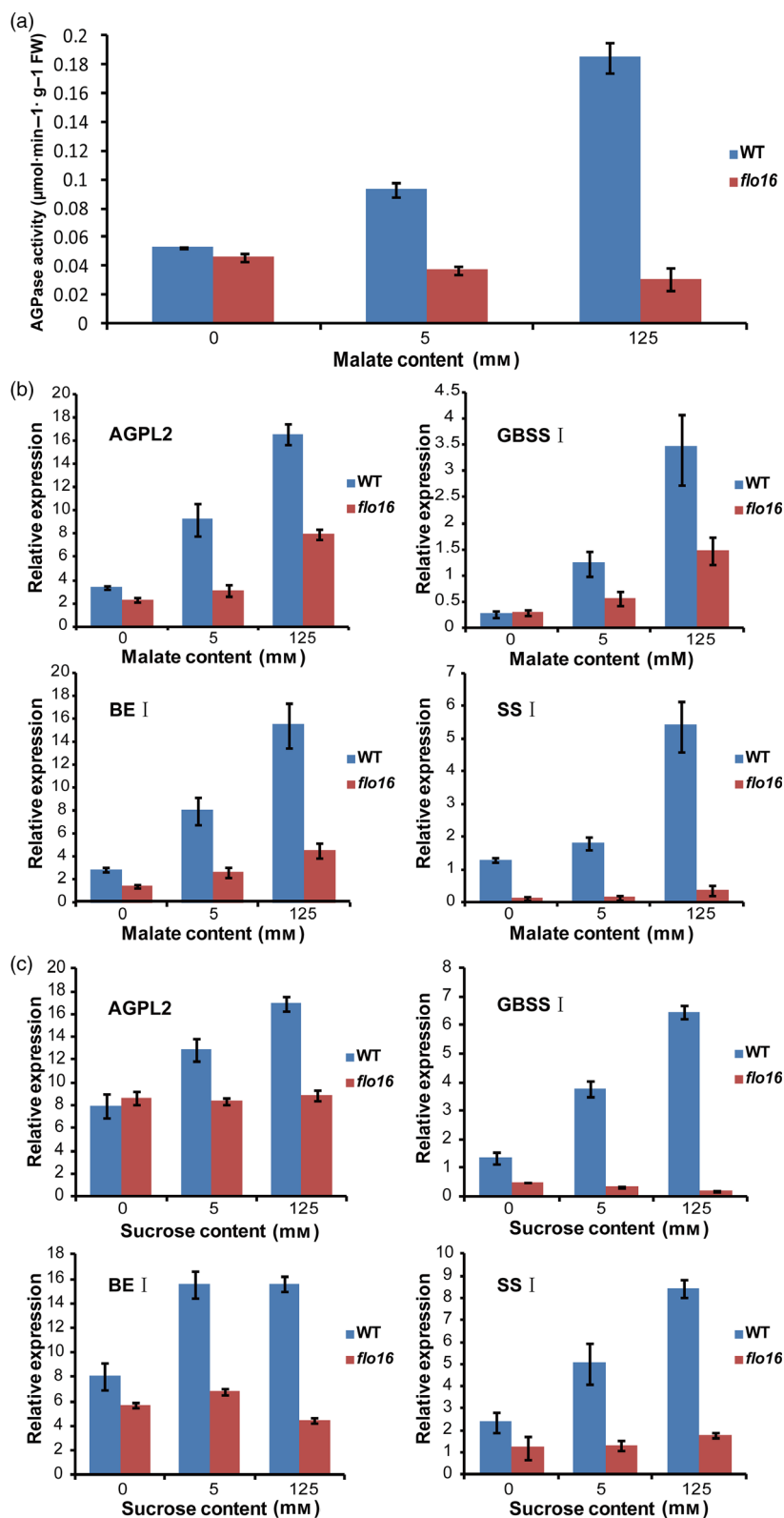


**Figure 8** Influence of exogenous malate and sucrose on starch synthesis enzymes in wild-type and *flo16* endosperm. (a) AGPase activities in wild-type and *flo16* developing endosperms at 9–12 DAF treated with malate. (b) Expression levels of starch synthesis enzymes in the developing endosperm at 9–12 DAF incubated in malate. (c) The Expression levels of starch synthesis enzymes in developing endosperm at 9–12 DAF treated with sucrose. Values are means  $\pm$  SD,  $n = 3$ .

Berkshire, UK). After sectioning with an ultramicrotome (UC7, Leica, Solms, Germany), specimens (1  $\mu$ m) were stained with I<sub>2</sub>-KI and observed under an optical microscope (Nikon, Tokyo, Japan).

Naturally fractured sections of mature seeds were observed with a scanning electron microscope (S-3400N, Hitachi, Tokyo, Japan) as described (Kang *et al.*, 2005).

#### Physicochemical properties of starch in endosperm

Starch content in the endosperm was measured using a starch assay kit (Megazyme, Ireland). Amylose, lipid and protein contents were measured as described previously (Kang *et al.*, 2005; Liu *et al.*, 2009). Chain length distribution of amylopectin



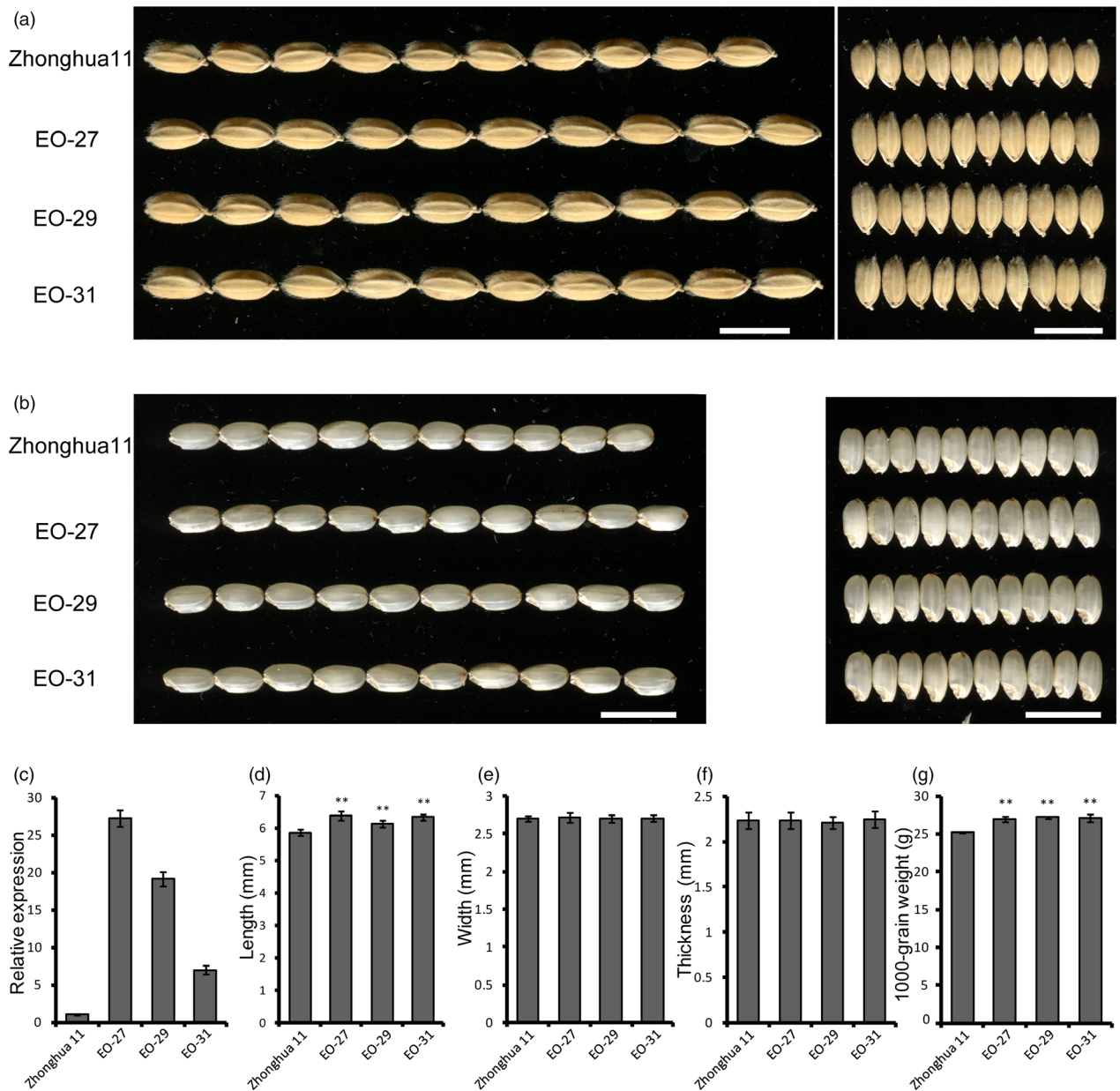


**Figure 9** Effects of endosperm-specific *FLO16* overexpression on grains. (a, b) Images of hulled (a) and dehulled (b) seeds of the recipient and transgenic lines. EO-27, EO-29 and EO-31 are independent transgenic lines. Scale bars, 1 cm. (c) Enhanced expression levels of *FLO16* in overexpression endosperms. Expression level in Zhonghua 11 was considered as sample control. Values are means  $\pm$  SDs,  $n = 3$ . (d–f) Size comparisons between the wild-type and transgenic seeds. Values are means  $\pm$  SDs,  $n = 10$ . (g) 1000-grain weights of overexpression lines. Values are means  $\pm$  SDs,  $n = 3$ . Asterisks indicate the statistical significance between the wild type and the mutant, determined by Student's *t*-tests (\*\* $P < 0.01$ ).

was measured using DSA-FACE (Han *et al.*, 2012). Pasting properties were determined with a rapid visco analyzer (RVA-Tec Master, Perten, Sweden). Gelatinization and swelling coefficient of starch were measured by mixing flour with different concentrations of urea (0–9 M) and incubating at 25°C for 24 h (Nishi *et al.*, 2001).

#### Mapping and cloning of *FLO16*

A total of 1502  $F_2$  individuals with recessive phenotype were used for map-based cloning. Molecular markers were developed according to nucleotide polymorphisms between N22 and DJY (Table S3). Six open reading frames (ORFs) in the fine-mapped

region were predicted by the Rice Annotation Project Database (<http://rapdb.dna.affrc.go.jp/>). The mutation was confirmed by sequencing PCR products for these genes.

#### Vector construction and plant transformation

For functional complementation of *flo16*, the wild-type *FLO16* sequence under control of its native promoter (2000 bp upstream of ATG) was inserted into vector pCubi1390. This plasmid was introduced into *flo16* callus by Agrobacterium-mediated transformation (Hiei and Komari, 2008; Hiei *et al.*, 1994). For endosperm-specific functional complementation of *flo16* and overexpression of *FLO16*, the wild-type *FLO16* sequence was

inserted into vector pCubi1390, in which *FLO16* was driven by the *Glutelin C* promoter. This plasmid was introduced into *flo16* and Zhonghua 11 callus, respectively. For constitutive overexpression of *FLO16*, the wild-type *FLO16* sequence was inserted into vector pCubi1390, in which *FLO16* was driven by the maize *Ubiquitin* promoter, and this plasmid was introduced into Zhonghua 11 callus. For promoter analysis, the *FLO16* promoter was inserted into a  $\beta$ -glucuronidase (*GUS*) expression vector and introduced into Nipponbare callus as described above. All primers used were listed in Table S4.

### GUS staining

Transgenic plants obtained as mentioned above were stained as described (Jefferson *et al.*, 1987). Images were captured with a stereoscope (Leica Application Suite 3.3, Germany)

### Subcellular localization

The coding sequence of *FLO16* was cloned into the pAN580-GFP vector to express *FLO16-GFP* under the control of a double 35S promoter. The control (*GFP* alone) and *FLO16-GFP* were each expressed in rice protoplasts (Chen *et al.*, 2006). Images of GFP fluorescence were captured using a confocal laser scanning microscope (LSM710, Zeiss, Germany).

### RNA extraction and qRT-PCR analysis

Total RNA was extracted using an RNA Prep Pure Plant kit (TIANGEN Biotech, Beijing). First-strand cDNA was synthesized from 2  $\mu$ g of total RNA by priming with oligo (dT) in 20  $\mu$ L reaction volumes, using a PrimeScript Reverse Transcriptase Kit (TaKaRa, Tokyo, Japan). qRT-PCR was performed using the SYBR Premix Ex Taq (TaKaRa) in an ABI7500 Real-time PCR system. Gene-specific primers used in this analysis are listed in Table S3 or the previous study (She *et al.*, 2010). *Actin1* was used as an internal control.

### Determination of metabolite levels

Levels of sucrose were quantified by UPLC as described previously (Fernie *et al.*, 2001). Malate contents were measured by enzymatic analysis (Nunes-Nesi *et al.*, 2007). ATP contents were detected using an ATP assay kit (Beyotime, Shanghai, China) according to the manufacturer's instructions. Developing grains and other tissues of rice were captured into liquid N<sub>2</sub> and stored in  $-80^{\circ}\text{C}$  if not extracted immediately, and all extractions were performed on ice as soon as possible to reduce loss of substance. Furthermore, the extractions for ATP and malate measurement were filtered across the 10 kDa ultrafiltration centrifugal tube (Millipore, Billerica, MA) to decrease degradation of the metabolites.

### Enzyme activity and zymogram analysis

Crude enzymes from developing endosperm were extracted for enzyme activity assays (Peng *et al.*, 2014). MDH isozymes were separated in 10% native polyacrylamide gels stained according to a previous study (Brown *et al.*, 1978). Total MDH activity assays were performed in reaction mixtures containing 10  $\mu$ L crude enzyme, 3 mM malate, 1 mM NAD buffered with 50 mM glycine-NaOH (pH 8.5) at 25°C and determined by monitoring altered NADH content at 340 nm (Zheng *et al.*, 2005). AGPase was extracted in 50 mM Hepes-KOH (pH 7.8) buffer with 5 mM MgCl<sub>2</sub> and analysed in 50 mM Hepes-KOH (pH 7.8), 5 mM MgCl<sub>2</sub>, 0.6 mM NAD, 2.5 mM Na-PPI, 1 unit/mL phosphoglucosyltransferase (Sigma-Aldrich, Saint Louis, MO), 2.5 units/mL Glc-6-P dehydrogenase (Sigma-Aldrich) and 1 mM ADP-Glc with or without 5 mM

DTT (Tiessen *et al.*, 2002). Activities measured with or without DTT were termed Vred or Vsel, respectively. Activities of starch synthases (SSI and SSIII) were determined according to Nishi *et al.* (2001). Phosphorylase (PHO1 and PHO2) activities were tested in a polyacrylamide gel containing 0.8% (w/v) oyster glycogen (Sigma-Aldrich) (Satoh *et al.*, 2008). All electrophoreses were conducted at 4°C.

### Incubation of endosperm discs with exogenous malate or sucrose

Developing seeds at 9–12 DAF were harvested and then sliced into 1-mm-thickness discs, washed three times in fresh incubation medium (50 mM HEPES-KOH, pH7.4), and incubated (~200 mg) in 5 mL of incubation medium containing Na-malate or sucrose in various concentration for 3 h. All incubations were performed at 30°C with 90 rpm shaking. After incubation, samples were washed three times in incubation medium and blotted with filter papers. Further assays were performed as mentioned above.

### Acknowledgements

This work was supported by the National Transgenic Science and Technology Program (2016ZX08009003-004), the National Natural Science Foundation of China (Grant 31330054), the Jiangsu Science and Technology Development Program (BE2017368), the Agricultural Science and Technology Innovation Fund project of Jiangsu Province (CX(16)1029) and the Fundamental Research Funds for the Central Universities (KYTZ201601). This work was also supported by the Key Laboratory of Biology, Genetics and Breeding of Japonica Rice in Mid-lower Yangtze River, Ministry of Agriculture, P.R. China, and the Jiangsu Collaborative Innovation Center for Modern Crop Production.

### References

- Ashikari, M., Sakakibara, H., Lin, S.Y., Yamamoto, T., Takashi, T., Nishimura, A., Angeles, E.R. *et al.* (2005) Cytokinin oxidase regulates rice grain production. *Science*, **309**, 741–745.
- Ball, S., Guan, H.P., James, M., Myers, A., Keeling, P., Mouille, G., Buleon, A. *et al.* (1996) From glycogen to amylopectin: a model for the biogenesis of the plant starch granule. *Cell*, **86**, 349–352.
- Beckles, D.M., Craig, J. and Smith, A.M. (2001) ADP-glucose pyrophosphorylase is located in the plastid in developing tomato fruit. *Plant Physiol.* **126**, 261–266.
- Beeler, S., Liu, H.C., Stadler, M., Schreier, T., Eicke, S., Lue, W.L., Truernit, E. *et al.* (2014) Plastidial NAD-dependent malate dehydrogenase is critical for embryo development and heterotrophic metabolism in *Arabidopsis*. *Plant Physiol.* **164**, 1175–1190.
- Berkemeyer, M., Scheibe, R. and Ocheretina, O. (1998) A novel, non-redox-regulated NAD-dependent malate dehydrogenase from chloroplasts of *Arabidopsis thaliana* L. *J. Biol. Chem.* **273**, 27927–27933.
- Brown, A.H.D., Nevo, E., Zohary, D. and Dagan, O. (1978) Genetic variation in natural populations of wild barley (*Hordeum spontaneum*). *Genetica*, **49**, 97–108.
- Centeno, D.C., Osorio, S., Nunes-Nesi, A., Bertolo, A.L., Carneiro, R.T., Araujo, W.L., Steinhäuser, M.C. *et al.* (2011) Malate plays a crucial role in starch metabolism, ripening, and soluble solid content of tomato fruit and affects postharvest softening. *Plant Cell*, **23**, 162–184.
- Chen, S.B., Tao, L.Z., Zeng, L.R., Vega-Sanchez, M.E., Umemura, K. and Wang, G.L. (2006) A highly efficient transient protoplast system for analyzing defence gene expression and protein-protein interactions in rice. *Mol. Plant Pathol.* **7**, 417–427.
- Fan, C.H., Xing, Y.Z., Mao, H.L., Lu, T.T., Han, B., Xu, C.G., Li, X.H. *et al.* (2006) GS3, a major QTL for grain length and weight and minor QTL for grain width

- and thickness in rice, encodes a putative transmembrane protein. *Theor. Appl. Genet.* **112**, 1164–1171.
- Fernie, A.R., Roscher, A., Ratcliffe, R.G. and Kruger, N.J. (2001) Fructose 2,6-bisphosphate activates pyrophosphate: fructose-6-phosphate 1-phosphotransferase and increases triose phosphate to hexose phosphate cycling in heterotrophic cells. *Planta*, **212**, 250–263.
- Gietl, C. (1992) Malate dehydrogenase isoenzymes: cellular locations and role in the flow of metabolites between the cytoplasm and cell organelles. *Biochem. Biophys. Acta.* **1100**, 217–234.
- Han, X.H., Wang, Y.H., Liu, X., Jiang, L., Ren, Y.L., Liu, F., Peng, C. et al. (2012) The failure to express a protein disulphide isomerase like protein results in a flouy endosperm and an endoplasmic reticulum stress response in rice. *J. Exp. Bot.* **63**, 121–130.
- Hanashiro, I., Tagawa, M., Shibahara, S., Iwata, K. and Takeda, Y. (2002) Examination of molar-based distribution of A, B and C chains of amylopectin by fluorescent labeling The failure to express a protein disulphide isomerase-like protein results in a flouy endosperm and an endoplasmic reticulum stress response in rice with 2-aminopyridine. *Carbohydr. Res.* **337**, 1211–1215.
- Hanashiro, I., Itoh, K., Kuratomi, Y., Yamazaki, M., Igarashi, T., Matsugasako, J.I. and Takeda, Y. (2008) Granule-bound starch synthase i is responsible for biosynthesis of extra-long unit chains of amylopectin in rice. *Plant Cell Physiol.* **49**, 925–933.
- Hebbelmann, I., Selinski, J., Wehmeyer, C., Goss, T., Voss, I., Mulo, P., Kangasjärvi, S. et al. (2012) Multiple strategies to prevent oxidative stress in Arabidopsis plants lacking the malate valve enzyme NADP-malate dehydrogenase. *J. Exp. Bot.* **63**, 1445–1459.
- Heber, U. (1974) Metabolite exchange between chloroplasts and cytoplasm. *Annu. Rev. Plant Physiol.* **25**, 393–421.
- Heng, Y.Q., Wu, C.Y., Long, Y., Luo, S., Ma, J., Chen, J., Liu, J.F. et al. (2018) OsALMT7 maintains panicle size and grain yield in rice by mediating malate transport. *Plant Cell*, **30**, 889–906.
- Heyno, E., Innocenti, G., Lemaire, S.D., Issakidis-Bourguet, E. and Krieger-Liszka, A. (2014) Putative role of the malate valve enzyme NADP-malate dehydrogenase in H<sub>2</sub>O<sub>2</sub> signalling in Arabidopsis. *Philos. Trans. R. Soc. B Biol. Sci.* **369**, 20130228–20130228.
- Hiei, Y. and Komari, T. (2008) Agrobacterium-mediated transformation of rice using immature embryos or calli induced from mature seed. *Nat. Protoc.* **3**, 824–834.
- Hiei, Y., Ohta, S., Komari, T. and Kumashiro, T. (1994) Efficient transformation of rice (*Oryza sativa* L.) mediated by Agrobacterium and sequence analysis of the boundaries of the T-DNA. *Plant J.* **6**, 271–282.
- Huang, X.Z., Qian, Q., Liu, Z.B., Sun, H.Y., He, S.Y., Luo, D., Xia, G.M. et al. (2009) Natural variation at the DEP1 locus enhances grain yield in rice. *Nat. Genet.* **41**, 494–497.
- Ishimaru, K., Hirotsu, N., Madoka, Y., Murakami, N., Hara, N., Onodera, H., Kashiwagi, T. et al. (2013) Loss of function of the IAA-glucose hydrolase gene TGW6 enhances rice grain weight and increases yield. *Nat. Genet.* **45**, 707–711.
- Isshiki, M., Nakajima, M., Satoh, H. and Shimamoto, K. (2000) dull: rice mutants with tissue-specific effects on the splicing of the waxy pre-mRNA. *Plant J.* **23**, 451–460.
- Isshiki, M., Matsuda, Y., Takasaki, A., Wong, H.L., Satoh, H. and Shimamoto, K. (2008) Du3, a mRNA cap-binding protein gene, regulates amylose content in Japonica rice seeds. *Plant Biotechnol.* **25**, 483–487.
- Jane, J.L., Kasemsuwan, T., Leas, S., Zobel, H. and Robyt, J.F. (1994) Anthology of starch granule morphology by scanning electron microscopy. *Starch*, **46**, 121–129.
- Jefferson, R.A., Kavanagh, T.A. and Bevan, M.W. (1987) GUS fusions: beta-glucuronidase as a sensitive and versatile gene fusion marker in higher plants. *EMBO J.* **6**, 3901–3907.
- Jiao, Y.Q., Wang, Y.H., Xue, D.W., Wang, J., Yan, M.X., Liu, G.F., Dong, G.J. et al. (2010) Regulation of OsSPL14 by OsmiR156 defines ideal plant architecture in rice. *Nat. Genet.* **42**, 541–544.
- Kang, H.G., Park, S., Matsuoka, M. and An, G. (2005) White-core endosperm flouy endosperm-4 in rice is generated by knockout mutations in the C-type pyruvate orthophosphate dikinase gene (OsPPDKB). *Plant J.* **42**, 901–911.
- Kromer, S. and Scheibe, R. (1996) Function of the chloroplastic malate valve for respiration during photosynthesis. *Biochem. Soc. Trans.* **24**, 761–766.
- Li, Y.B., Fan, C.C., Xing, Y.Z., Jiang, Y.H., Luo, L.J., Sun, L., Shao, D. et al. (2011) Natural variation in GS5 plays an important role in regulating grain size and yield in rice. *Nat. Genet.* **43**, 1266–1269.
- Li, Y.B., Fan, C.C., Xing, Y.Z., Yun, P., Luo, L.J., Yan, B., Peng, B. et al. (2014) Chalk5 encodes a vacuolar H<sup>+</sup>-translocating pyrophosphatase influencing grain chalkiness in rice. *Nat. Genet.* **46**, 657–657.
- Li, S.F., Wei, X.J., Ren, Y.L., Qiu, J.H., Jiao, G.A., Guo, X.P., Tang, S.Q. et al. (2017) OsBT1 encodes an ADP-glucose transporter involved in starch synthesis and compound granule formation in rice endosperm. *Sci. Rep.* **7**, 40124.
- Liu, L., Ma, X., Liu, S., Zhu, C., Jiang, L., Wang, Y., Shen, Y. et al. (2009) Identification and characterization of a novel Waxy allele from a Yunnan rice landrace. *Plant Mol. Biol.* **71**, 609–626.
- Liu, J.F., Chen, J., Zheng, X.M., Wu, F.Q., Lin, Q.B., Heng, Y.Q., Tian, P. et al. (2017) GW5 acts in the brassinosteroid signalling pathway to regulate grain width and weight in rice. *Nat. Plant* **3**, 17043.
- Long, W.H., Dong, B.N., Wang, Y.H., Pan, P.Y., Wang, Y.L., Liu, L.L., Chen, X.L. et al. (2017) FLOURY ENDOSPERM8, encoding the UDP-glucose pyrophosphorylase 1, affects the synthesis and structure of starch in rice endosperm. *J. Plant Biol.* **60**, 513–522.
- Mao, H.L., Sun, S.Y., Yao, J.L., Wang, C.R., Yu, S.B., Xu, C.G., Li, X.H. et al. (2010) Linking differential domain functions of the GS3 protein to natural variation of grain size in rice. *Proc. Natl Acad. Sci. USA* **107**, 19579–19584.
- Martin, C. and Smith, A.M. (1995) Starch biosynthesis. *Plant Cell*, **7**, 971–985.
- Matsushima, R., Maekawa, M., Fujita, N. and Sakamoto, W. (2010) A rapid, direct observation method to isolate mutants with defects in starch grain morphology in rice. *Plant Cell Physiol.* **51**, 728–741.
- Matsushima, R., Maekawa, M., Kusano, M., Kondo, H., Fujita, N., Kawagoe, Y. and Sakamoto, W. (2014) Amyloplast-localized SUBSTANDARD STARCH GRAIN4 protein influences the size of starch grains in rice endosperm. *Plant Physiol.* **164**, 623–636.
- Matsushima, R., Maekawa, M., Kusano, M., Tomita, K., Kondo, H., Nishimura, H., Crofts, N. et al. (2016) Amyloplast membrane protein SUBSTANDARD STARCH GRAIN6 controls starch grain size in rice endosperm. *Plant Physiol.* **170**, 1445–1459.
- Nakamura, Y. (2002) Towards a better understanding of the metabolic system for amylopectin biosynthesis in plants: rice endosperm as a model tissue. *Plant Cell Physiol.* **43**, 718–725.
- Nishi, A., Nakamura, Y., Tanaka, N. and Satoh, H. (2001) Biochemical and genetic analysis of the effects of amylose-extender mutation in rice endosperm. *Plant Physiol.* **127**, 459–472.
- Nishio, T. and Iida, S. (1993) Mutants having a low content of 16-kDa allergenic protein in rice (*Oryza sativa* L.). *Theor. Appl. Genet.* **86**, 317–321.
- Nunes-Nesi, A., Carrari, F., Gibon, Y., Sulpice, R., Lytovchenko, A., Fisahn, J., Graham, J. et al. (2007) Deficiency of mitochondrial fumarate activity in tomato plants impairs photosynthesis via an effect on stomatal function. *Plant J.* **50**, 1093–1106.
- Peng, C., Wang, Y.H., Liu, F., Ren, Y.L., Zhou, K.N., Lv, J., Zheng, M. et al. (2014) FLOURY ENDOSPERM6 encodes a CBM48 domain-containing protein involved in compound granule formation and starch synthesis in rice endosperm. *Plant J.* **77**, 917–930.
- Pracharoenwattana, I., Zhou, W. and Smith, S.M. (2010) Fatty acid beta-oxidation in germinating Arabidopsis seeds is supported by peroxisomal hydroxypyruvate reductase when malate dehydrogenase is absent. *Plant Mol. Biol.* **72**, 101–109.
- Qi, P., Lin, Y.S., Song, X.J., Shen, J.B., Huang, W., Shan, J.X., Zhu, M.Z. et al. (2012) The novel quantitative trait locus GL3.1 controls rice grain size and yield by regulating Cyclin-T1;3. *Cell Res.* **22**, 1666–1680.
- Qiao, Y., Lee, S.I., Piao, R., Jiang, W., Ham, T.H., Chin, J.H., Piao, Z. et al. (2010) Fine mapping and candidate gene analysis of the flouy endosperm gene, FLO (a), in rice. *Mol. Cell* **29**, 167–174.
- Ryoo, N., Yu, C., Park, C.S., Baik, M.Y., Park, I.M., Cho, M.H., Bho, S.H. et al. (2007) Knockout of a starch synthase gene OsSIIIa/Flo5 causes white-core flouy endosperm in rice (*Oryza sativa* L.). *Plant Cell Rep.* **26**, 1083–1095.
- Satoh, H., Shibahara, K., Tokunaga, T., Nishi, A., Tasaki, M., Hwang, S.K., Okita, T.W. et al. (2008) Mutation of the plastidial alpha-glucan



- phosphorylase gene in rice affects the synthesis and structure of starch in the endosperm. *Plant Cell* **20**, 1833–1849.
- Scheibe, R. (1987) NADP<sup>+</sup>-malate dehydrogenase in C3-plants: regulation and role of a light-activated enzyme. *Physiol. Plant.* **71**, 393–400.
- Scheibe, R. (2004) Malate valves to balance cellular energy supply. *Physiol. Plant.* **120**, 21–26.
- Sew, Y.S., Stroher, E., Fenske, R. and Millar, A.H. (2016) Loss of mitochondrial malate dehydrogenase activity alters seed metabolism impairing seed maturation and post-germination growth in Arabidopsis. *Plant Physiol.* **171**, 849–863.
- She, K.C., Kusano, H., Koizumi, K., Yamakawa, H., Hakata, M., Imamura, T., Fukuda, M. *et al.* (2010) A novel factor FLOURY ENDOSPERM2 is involved in regulation of rice grain size and starch quality. *Plant Cell* **22**, 3280–3294.
- Shomura, A., Izawa, T., Ebana, K., Ebitani, T., Kanegae, H., Konishi, S. and Yano, M. (2008) Deletion in a gene associated with grain size increased yields during rice domestication. *Nat. Genet.* **40**, 1023–1028.
- Song, X.J., Huang, W., Shi, M., Zhu, M.Z. and Lin, H.X. (2007) A QTL for rice grain width and weight encodes a previously unknown RING-type E3 ubiquitin ligase. *Nat. Genet.* **39**, 623–630.
- Sullivan, T.D., Strelow, L.I., Illingworth, C.A., Phillips, R.L. and Nelson, O.E. Jr. (1991) Analysis of maize brittle-1 alleles and a defective suppressor-mutator-induced mutable allele. *Plant Cell* **3**, 1337–1348.
- Szeczowka, M., Osorio, S., Obata, T., Araujo, W.L., Rohrmann, J., Nunes-Nesi, A. and Fernie, A.R. (2012) Decreasing the mitochondrial synthesis of malate in potato tubers does not affect plastidial starch synthesis, suggesting that the physiological regulation of ADPglucose pyrophosphorylase is context dependent. *Plant Physiol.* **160**, 2227–2238.
- Taniguchi, M. and Miyake, H. (2012) Redox-shuttling between chloroplast and cytosol: Integration of intra-chloroplast and extrachloroplast metabolism. *Curr. Opin. Plant Biol.* **15**, 252–260.
- Tateoka, T. (1962) Starch grains of endosperm in grass systematics. *Bot. Soc. Japan* **75**, 377–383.
- Tetlow, I.J., Davies, E.J., Vardy, K.A., Bowsher, C.G., Burrell, M.M. and Emes, M.J. (2003) Subcellular localization of ADPglucose pyrophosphorylase in developing wheat endosperm and analysis of the properties of a plastidial isoform. *J. Exp. Bot.* **54**, 715–725.
- Tetlow, I.J., Wait, R., Lu, Z., Akkasaeng, R., Bowsher, C.G., Esposito, S., Kosar-Hashemi, B. *et al.* (2004) Protein phosphorylation in amyloplasts regulates starch branching enzyme activity and protein-protein interactions. *Plant Cell* **16**, 694–708.
- Tetlow, I.J., Beisel, K.G., Cameron, S., Makhmoudova, A., Liu, F., Bresolin, N.S., Wait, R. *et al.* (2008) Analysis of protein complexes in wheat amyloplasts reveals functional interactions among starch biosynthetic enzymes. *Plant Physiol.* **146**, 1878–1891.
- Tiessen, A., Hendriks, J.H., Stitt, M., Branscheid, A., Gibon, Y., Farre, E.M. and Geigenberger, P. (2002) Starch synthesis in potato tubers is regulated by post-translational redox modification of ADP-glucose pyrophosphorylase: a novel regulatory mechanism linking starch synthesis to the sucrose supply. *Plant Cell*, **14**, 2191–2213.
- Tomaz, T., Bagard, M., Pracharoenwattana, I., Linden, P., Lee, C.P., Carroll, A.J., Stroher, E. *et al.* (2010) Mitochondrial malate dehydrogenase lowers leaf respiration and alters photorespiration and plant growth in Arabidopsis. *Plant Physiol.* **154**, 1143–1157.
- Tuncel, A., Cakir, B., Hwang, S.K. and Okita, T.W. (2014) The role of the large subunit in redox regulation of the rice endosperm ADP-glucose pyrophosphorylase. *FEBS J.* **281**, 4951–4962.
- Wang, S.J., Yeh, K.W. and Tsai, C.Y. (2001) Regulation of starch granule-bound starch synthase I gene expression by circadian clock and sucrose in the source tissue of sweet potato. *Plant Sci.* **161**, 635–644.
- Wang, S.K., Wu, K., Yuan, Q.B., Liu, X.Y., Liu, Z.B., Lin, X.Y., Zeng, R.Z. *et al.* (2012) Control of grain size, shape and quality by OsSPL16 in rice. *Nat. Genet.* **44**, 950–954.
- Wang, S.K., Li, S., Liu, Q., Wu, K., Zhang, J.Q., Wang, S.S., Wang, Y. *et al.* (2015a) The OsSPL16-GW7 regulatory module determines grain shape and simultaneously improves rice yield and grain quality. *Nat. Genet.* **47**, 949–954.
- Wang, Y.X., Xiong, G.S., Hu, J., Jiang, L., Yu, H., Xu, J., Fang, Y.X. *et al.* (2015b) Copy number variation at the GL7 locus contributes to grain size diversity in rice. *Nat. Genet.* **47**, 944–948.
- Weng, J.F., Gu, S.H., Wan, X.Y., Gao, H., Guo, T., Su, N., Lei, C.L. *et al.* (2008) Isolation and initial characterization of GW5, a major QTL associated with rice grain width and weight. *Cell Res.* **18**, 1199–1209.
- Zeng, D., Yan, M.X., Wang, Y.H., Liu, X.F., Qian, Q. and Li, J.Y. (2007) Du1, encoding a novel Prp1 protein, regulates starch biosynthesis through affecting the splicing of Wx(b) supercript stop pre-mRNAs in rice (*Oryza sativa* L.). *Plant Mol. Biol.* **65**, 501–509.
- Zhang, X.J., Wang, J.F., Huang, J., Lan, H.X., Wang, C.L., Yin, C.F., Wu, Y.Y. *et al.* (2012) Rare allele of OsPPKL1 associated with grain length causes extra-large grain and a significant yield increase in rice. *Proc. Natl Acad. Sci. USA* **109**, 21534–21539.
- Zhang, L., Ren, Y.L., Lu, B.Y., Yang, C.Y., Feng, Z.M., Liu, Z., Chen, J. *et al.* (2016) FLOURY ENDOSPERM7 encodes a regulator of starch synthesis and amyloplast development essential for peripheral endosperm development in rice. *J. Exp. Bot.* **67**, 633–647.
- Zheng, N., Xu, J., Wu, Z., Chen, J., Hu, X., Song, L., Yang, G. *et al.* (2005) Clonorchis sinensis: molecular cloning and functional expression of novel cytosolic malate dehydrogenase. *Exp. Parasitol.* **109**, 220–227.

## Supporting information

Additional supporting information may be found online in the Supporting Information section at the end of the article.

**Figure S1** Endosperm-specific functional complementation lines of *flo16* restore normal appearance.

**Figure S2** NADP<sup>+</sup>/NADPH and ATP contents in developing endosperm.

**Figure S3** Metabolic differences between wild type and *flo16* in young seedling.

**Figure S4** Redox activation state of AGPase.

**Figure S5** Effects of *FLO16* over-expression on grains.

**Table S1** Comparison of agronomic traits between the wild type and *flo16* mutant.

**Table S2** Agronomic traits of overexpression lines.

**Table S3** Oligonucleotide primers used in map-based cloning.

**Table S4** Gene-specific primers used in this study.